Available online at www.sciencedirect.com
ScienceDirect
Journal of Power Sources 167 (2007) 265–271
JOURNAL OF POWER SOURCES
www.elsevier.com/locate/jpowsour

Simultaneous oxygen-reduction and methanol-oxidation reactions at the cathode of a DMFC: A model-based electrochemical impedance spectroscopy study

C.Y. Du, T.S. Zhao *, C. Xu

Department of Mechanical Engineering, The Hong Kong University of Science and Technology, Clear Water Bay, Kowloon, Hong Kong SAR, China

Received 12 January 2007; received in revised form 16 February 2007; accepted 19 February 2007
Available online 1 March 2007

Abstract

A model-based electrochemical impedance spectroscopy (EIS) approach that combines an equivalent electrical circuit (EEC) method and a mathematical model derived from the reaction kinetics is proposed to investigate the simultaneous oxygen-reduction reaction (ORR) and methanol-oxidation reaction (MOR) at the cathode of a DMFC. Good agreements between the calculated results and the experimental data validated the proposed method. Detailed kinetic parameters and state variables of the cathode were conveniently extracted and the concerned reaction processes were further analyzed, which demonstrated the comprehensive applicability of this method. The results showed a significant poisoning effect on the ORR by the presence of methanol at the cathode. The results also indicated that whether the methanol permeated from the anode can be completely oxidized by electrochemical reaction at the DMFC cathode depends on the electrode design and operating conditions, even at high potentials.

Keywords: DMFC; Cathode; Methanol crossover; EIS; Model

1. Introduction

Methanol crossover, the permeation of methanol through the ionomer membrane from the anode to the cathode, results in simultaneous cathodic oxygen-reduction reaction (ORR) and anodic methanol-oxidation reaction (MOR) at the cathode of a direct methanol fuel cell (DMFC). The simultaneous MOR and ORR lead to not only a fuel loss, but also a decrease in the cathode potential, which is one of major problems for DMFC performance [1–3]. To suppress the effect of the permeated methanol, it is essential to gain better understanding of the mechanism of how the MOR interacts with the ORR and how this interaction lowers the cathode potential. Recently, to understand the mechanism of the simultaneous MOR and ORR, extensive investigations have been reported by using traditional electrochemical and spectroscopic methods [1–8]. Despite a significant progress made, the kinetics of simultaneous MOR and ORR at the DMFC cathode is still not well understood, mainly due to the complicated nature of the reactions involving multi-step kinetics, and hence further studies are needed.

Electrochemical impedance spectroscopy (EIS) is a powerful tool for elucidating reaction mechanisms involving multi-step kinetics, because it has the advantage of separating different rate processes in the frequency domain, and therefore provides a better insight on the interfacial processes and species in electrochemical systems. Up to now, however, only little attention has been paid to the application of EIS to the investigation of the DMFC cathode behavior [9–13]. Müller and Urban [9] firstly introduced a method of obtaining DMFC cathode impedance spectra based on recording individually the impedance data for the entire DMFC and the anode only, followed by the calculation of the DMFC cathode impedance. Using the same procedure, Piela et al. [10] measured and gave some further interpretation of the cathode impedance spectra. Also, aiming to examine transport and reaction kinetics, some reference electrode methods were adopted to measure the cathode impedance spectra individually [11–13]. These pioneering EIS investigations are greatly helpful in understanding the cathode behavior. However, partly because of the complexity of the impedance data, all these investigations used the equivalent electrical circuit (EEC) method, in

* Corresponding author. Tel.: +852 2358 8647; fax: +852 2358 1543.
E-mail address: metzhao@ust.hk (T.S. Zhao).

0378-7753/$ – see front matter © 2007 Elsevier B.V. All rights reserved.
doi:10.1016/j.jpowsour.2007.02.048

which the obtained parameters may not have physical equivalents, and therefore, it is difficult to extract detailed information about the electrode reaction mechanism [14]. In addition, for a given impedance spectra, there may be several EECs that can all provide a good fitting, making it difficult to select the proper EEC model for the studied electrode system.

In this work, we propose a model-based EIS approach, which combines the EEC method and a mathematical model established from the detailed reaction mechanism, and apply this approach to investigate the simultaneous MOR and ORR at the DMFC cathode. This method can avoid the problems of the only EEC method, and more importantly, provide very detailed reaction information, e.g. the kinetic parameters and state variables. To the best of our knowledge, this is the first attempt to study the DMFC cathode by a model-based EIS method. We started with a mathematical derivation of the Faradaic impedance, based on a simplified reaction mechanism for the simultaneous MOR and ORR, and established a relationship between the Faradaic impedance and a general EEC. Then, the experimental impedance data were measured by a half-cell method. Finally, from the established relationship and the measured experimental data, the specific kinetic parameters and state variables for the simultaneous MOR and ORR were extracted and the results were analyzed based on the extracted parameters.

2. Theoretical

As discussed below, simultaneous MOR and ORR that occur at the cathode of a DMFC involve two adsorbed species. Based on the state variable theory [15,16], the Faradaic impedance (Z_F) for such an electrode process can be expressed as [17,18]:

$$Z_F = \frac{1}{(1/R_t) + (A + j\omega B)/(D - \omega^2 + j\omega T)} \quad (1)$$

where ω is the radial frequency,

$$\frac{1}{R_t} = \frac{\partial I_F}{\partial E} \quad (2)$$

with I_F and E representing the Faradaic current density and the electrode potential, respectively,

$$A = m_1 J_{12} n_2 + m_2 J_{21} n_1 - m_1 J_{22} n_1 - m_2 J_{11} n_2 \quad (3)$$

$$B = m_1 n_1 + m_2 n_2 \quad (4)$$

$$D = J_{11} J_{22} - J_{12} J_{21} \quad (5)$$

$$T = -J_{11} - J_{22} \quad (6)$$

with

$$m_i = \frac{\partial I_F}{\partial \theta_i} \quad i = 1, 2 \quad (7)$$

$$n_i = \frac{\partial \dot{\theta}_i}{\partial E} \quad i = 1, 2 \quad (8)$$

$$J_{ik} = \frac{\partial \dot{\theta}_i}{\partial \dot{\theta}_k} \quad i, k = 1, 2 \quad (9)$$

where θ_i and $\dot{\theta}_i$ are respective adsorbate coverage and its change rate with time.

Apparently, to determine Z_F as a function of ω at a fixed potential E, the relationship between I_F, θ_i, $\dot{\theta}_i$, and E has to be identified to extract the parameter values for impedance calculation. To this end, a simple reaction mechanism for simultaneous MOR and ORR is employed:

$$Pt + CH_3OH \xrightarrow{k_1} Pt - CO_{ads} + 4H^+ + 4e^- \quad (10)$$

$$Pt - CO_{ads} + H_2O \xrightarrow{k_2} Pt + CO_2 + 2H^+ + 2e^- \quad (11)$$

$$Pt + O_2 + H^+ + e^- \xrightarrow{k_3} Pt - O_2H_{ads} \quad (12)$$

$$Pt - O_2H_{ads} + 3H^+ + 3e^- \underset{k_{-4}}{\overset{k_{+4}}{\rightleftharpoons}} Pt + 2H_2O \quad (13)$$

The electro-catalytic oxidation of methanol involves two series steps [19,20]. The first step is the adsorption and dehydration of methanol to form the absorbed CO species. The second step represents the irreversible oxidation of the CO species, leading to CO_2 evolution. Oxygen reduction on Pt under acidic media is usually characterized by the two-step Damjanovic mechanism [21,22]. The first step is an electrochemical step corresponding to the protonation of the O_2, which is the rate-determining step. Then the formed adsorption species, O_2H, is further reduced to water. The reaction rates v_i ($i = 1, 2, 3, 4$) corresponding to the Eqs. (10)–(13) can be expressed as:

$$v_1 = k_1 c_1 (1 - \theta_1 - \theta_2) \exp\left(\frac{E}{b_1}\right) \quad (14)$$

$$v_2 = k_2 \theta_1 \exp\left(\frac{E}{b_2}\right) \quad (15)$$

$$v_3 = k_3 c_2 (1 - \theta_1 - \theta_2) \exp\left(-\frac{E}{b_3}\right) \quad (16)$$

$$v_4 = k_{+4} \theta_2 \exp\left(-\frac{E}{b_4}\right) - k_{-4}(1 - \theta_1 - \theta_2) \exp\left(\frac{E}{b_4}\right) \quad (17)$$

where k_i ($i = 1, 2, 3, +4, -4$) are rate constants, b_i ($i = 1, 2, 3, 4$) the Tafel slopes, θ_1 and θ_2 the coverage of CO and O_2H, c_1 and c_2 the concentrations of methanol and oxygen. Based on the proposed reaction mechanism (Eqs. (10)–(13)), the Faradaic current density (I_F) can be written as:

$$I_F = F(4v_1 + 2v_2 - v_3 - 3v_4) \quad (18)$$

where F is the Faradaic constant. According to mass balance, the change rates of absorbate coverage ($\dot{\theta}_i$) is the net result of production and consumption of the absorbates, and can be expressed as:

$$\dot{\theta}_1 = \frac{d\theta_1}{dt} = \frac{F}{q_1}(v_1 - v_2) \quad (19)$$

$$\dot{\theta}_2 = \frac{d\theta_2}{dt} = \frac{F}{q_2}(v_3 - v_4) \quad (20)$$

where q_1 (420 $\mu C\,cm^{-2}$ [14]) and q_2 (assumed 420 $\mu C\,cm^{-2}$) are the charges required for complete CO and O_2H adsorption on unit Pt surface.

By substituting I_F, θ_i and $\dot{\theta}_i$ into Eqs. (2)–(9) with the expressions in Eqs. (14)–(20), the relationships between R_t, A, B, D, T and the kinetic and state parameters (k_i, b_i, θ_i and c_i) can be established.

According to Wu et al. [18], the Faradaic impedance for an electrode process with two adsorbed species can also be expressed by a general EEC, shown in Fig. 1a, and thus, the mathematical expression of the Faradaic impedance can be equivalently written as

$$Z_F = R_t + \sum_{i=1}^{2} \frac{R_i}{1 + j\omega R_i C_i} \quad i = 1, 2 \tag{21}$$

where R_i is the resistance elements, C_i the capacitance elements. Comparing the Eq. (1) with the Eq. (21), the relationship between the electrical elements in the EEC and the electrochemical parameters in the Faradaic impedance expression Eq. (1) can be established as:

$$A = -\frac{1}{R_t^2}\left(\frac{R_1 + R_2}{R_1 R_2 C_1 C_2}\right) \tag{22}$$

$$B = -\frac{1}{R_t^2}\left(\frac{1}{C_1} + \frac{1}{C_2}\right) \tag{23}$$

$$D = \frac{1}{R_1 R_2 C_1 C_2} - R_t A \tag{24}$$

$$T = \frac{R_1 C_1 + R_2 C_2}{R_1 R_2 C_1 C_2} - R_t B \tag{25}$$

From Eqs. (22)–(25), the electrochemical parameters A, B, D and T can be calculated from the values of the electrical elements R_t, R_i and C_i, which can be obtained by fitting experimental data with the proposed EEC. Also, as was mentioned above, A, B, D and T as well as R_t are related to the kinetic and state parameters (k_i, b_i, θ_i and c_i) of the simultaneous MOR and ORR kinetics. Therefore, based on Eqs. (2)–(6), the kinetic and state parameters (k_i, b_i, θ_i and c_i) can be obtained from the calculated A, B, D, T and R_t by a simplex nonlinear regression procedure.

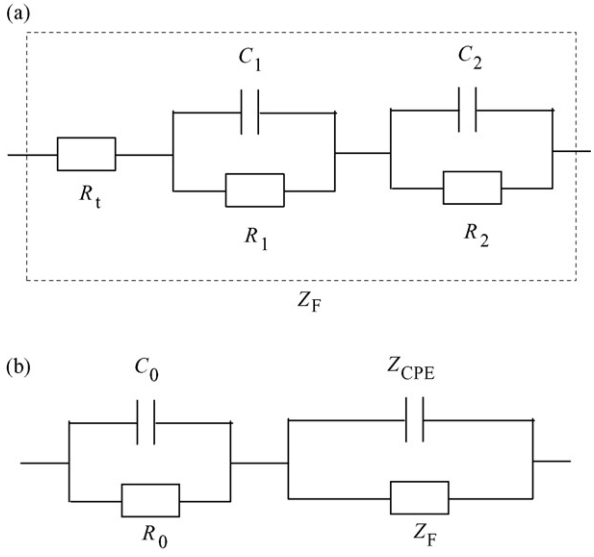

Fig. 1. Equivalent electrical circuit for the evaluation of impedance responses of the DMFC cathode: (a) Faradic impedance for an electrode reaction with two absorption intermediates, and (b) a complete circuit model for the DMFC cathode.

3. Experimental

The experimental impedance spectra of the DMFC cathode were measured by a half-cell method, which was proved reliable for EIS measurement [23–25]. In this half cell, a half membrane electrode assembly (MEA), consisting of a Nafion membrane with a gas diffusion electrode (GDE) on one side, was held vertically. The GDE, consisting of a catalyst layer and a gas diffusion layer, was in contact with a flow field plate, through which O_2 was supplied and electric current was extracted. The membrane was exposed to the electrolyte solution, in which a platinum mesh was immersed to serve as a counter electrode. A saturated calomel electrode (SCE) was positioned approximately 4.0 mm away from the membrane via a Luggin capillary to serve as a reference electrode. The half-MEA was obtained by hot-pressing a Nafion 112 membrane and a 1 cm^2 in-house GDE with Pt loading 0.1 mg cm^{-2}. The in-house fabricated GDE was prepared by spraying a catalyst ink consisting of 60 wt.% Pt/C catalyst, 5 wt.% Nafion solution and ethanol onto a wet-proofed carbon cloth substrate.

All the electrochemical measurements were conducted in deaerated 0.5 M H_2SO_4 + 0.5 M CH_3OH solution at ambient temperature (20 °C), using an Autolab PGSTAT 30 with a frequency response analyzer module, FRA2. A high flow rate of unhumidified O_2 (100 sccm) at atmospheric pressure was adopted to eliminate the mass-transport limitations of oxygen and keep the ORR almost under pure kinetic control. The impedance spectra were recorded 10 points/decade in the potentiostatic mode by sweeping frequencies from 50k to 0.02 Hz range at an amplitude of 10 mV.

4. Results and discussion

Fig. 2 shows the experimental EIS patterns of the electrode at various potentials. At high frequencies, the impedance showed a line with a slope close to 45°. This line, apparently independent of the electrode potential, could be ascribed to the ionic ohmic drop in the membrane or the electronic contact between different layers [21,26]. At medium frequencies, a large capacitive arc was observed, which was associated with the charge transfer processes [27] and depressed due to a high roughness of the electrode. At low frequencies, there was an unobvious pseudo inductive loop. Such pseudo inductive patterns, which are typical features of systems with adsorbed intermediates [28], are critical to proposing the reaction kinetics and the fitting EEC for the DMFC cathode.

Considering the measured impedance patterns, the reaction mechanism, and the structural features of the half cell, the experimental data in Fig. 2 were fitted by a proposed EEC shown in Fig. 1b, where R_0 is the membrane or contact resistance, C_0 the membrane or contact capacitance, Z_{CPE} the constant phase element (CPE), and Z_F the Faradaic impedance as presented in Fig. 1a. In this EEC, the parallel combination of R_0 and C_0 was

Table 1
Fitted values of the elements in the equivalent electrical circuit illustrated in Fig. 1

E (V)	Y (F m^{-2})	α	R_0 (Ω m^2)	C_0 (F m^{-2})	R_t (Ω m^2)	R_1 (Ω m^2)	C_1 (F m^{-2})	R_2 (Ω m^2)	C_2 (F m^2)
0.75	0.1119	0.7997	0.00156	0.01148	0.10480	0.16080	0.03190	−0.01412	−19.01
0.71	0.1031	0.8275	0.00156	0.01408	0.07910	0.08720	0.03611	−0.01030	−15.73
0.68	0.1101	0.8010	0.00155	0.01267	0.05008	0.06852	0.03874	−0.007580	−14.92
0.65	0.1187	0.7910	0.00159	0.01533	0.04246	0.04712	0.04637	−0.006090	−12.68

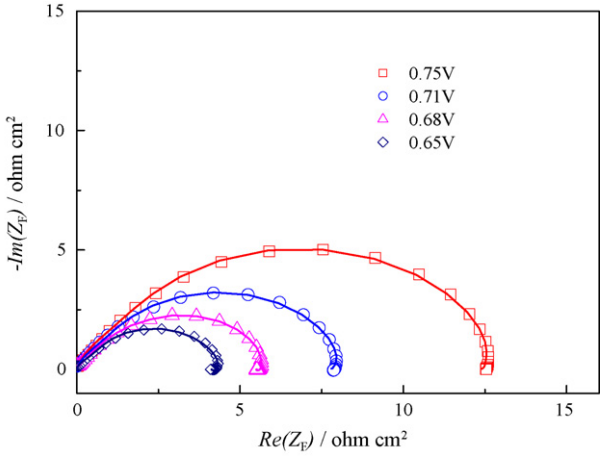

Fig. 2. Complex-plane impedance patterns of the electrode at various potentials. Scattered points: experimental data; solid line: the fitted data by the equivalent circuit illustrated in Fig. 1.

used to fit the ionic ohmic drop in the membrane or the electronic contact between different layers. The CPE, instead of a pure capacitor, was used for the electric double-layer capacitance to account for the electrode roughness. The impedance of a CPE can be written as

$$Z_{\mathrm{CPE}} = \frac{1}{Y(\mathrm{j}\omega)^{\alpha}} \tag{26}$$

where Y is the magnitude and α the dimensionless parameter which has a value from −1 to 1. The fitted results using the above EEC are listed in Table 1 and the simulated EIS patterns with these fitted results are shown in Fig. 2, in which a good agreement with the experimental data was observed. Based on the established correlations (Eqs. (22)–(25)), the electrochemical parameters A, B, D and T in the mathematical expression of Faradaic impedance (Eq. (1)) at various potentials were then calculated from the fitted values of the electrical elements and are given in Table 2.

After obtaining the electrochemical parameters in the Faradaic impedance expression, the specific kinetic parameters and state variables for the simultaneous MOR and ORR mechanism

Table 2
Calculated values of the electrochemical parameters in Eq. (1)

E (V)	A (Ω^{-1} m^{-2} s^{-2})	B (Ω^{-1} m^{-2} s^{-2})	D (s^{-2})	T (s^{-1})
0.75	-9.70×10^3	-2.85×10^3	1.74×10^3	497.3
0.71	-2.17×10^4	-3.97×10^3	3.48×10^3	606.5
0.68	-8.09×10^4	-1.03×10^4	7.38×10^3	899.7
0.65	-1.35×10^5	-1.19×10^4	1.17×10^4	976.7

Table 3
Fitted kinetic parameters for the simultaneous MOR and ORR.

Parameters	Values
k_1 (mol s^{-1} m^{-2})	2.86×10^{-8}
k_2 (mol s^{-1} m^{-2})	6.48×10^{-11}
k_3 (mol s^{-1} m^{-2})	0.28
k_{+4} (mol s^{-1} m^{-2})	88.70
k_{-4} (mol s^{-1} m^{-2})	3.96×10^{-8}
b_1 (V dec^{-1})	0.058
b_2 (V dec^{-1})	0.069
b_3 (V dec^{-1})	0.053
b_4 (V dec^{-1})	0.062

were extracted by a nonlinear fitting procedure based on the established correlations (Eqs. (2)–(6)). Table 3 summarizes the fitted kinetic parameters for the simultaneous MOR and ORR. For MOR, k_2 is almost two orders of magnitude lower than k_1, indicating oxidation of the absorbed CO was the rate-determining step whereas adsorption of the methanol molecule to form the CO species was relatively faster. For ORR, k_3 is significantly lower than k_{+4}, indicating the oxygen reduction to the absorbed O_2H was the rate-determining step, which was in agreement with the previous assumption for the ORR.

The coverage of the absorbed species at a DMFC cathode, which is often obtained by complicated spectroscopic apparatuses, could also be obtained by our model-based EIS method. Fig. 3 presents the calculated values of CO and O_2H coverage, as well as the free surface, as a function of the electrode potential. With the increase in potential, θ_1 decreased whereas θ_2 increased steadily. From 0.65 to 0.75 V, θ_1 decreased from about 0.7 to 0.1 and θ_2 increased from 0.3 to 0.8. The continuous declining of θ_1 could be interpreted by the electro-oxidative removal of

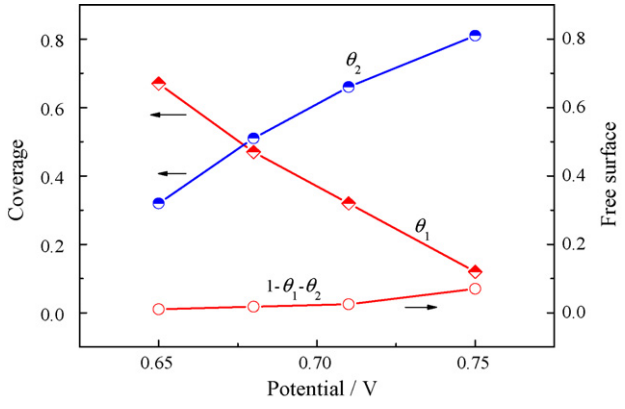

Fig. 3. Calculated CO and O_2H coverage (θ_1 and θ_2) and free surface ($1-\theta_1-\theta_2$) as a function of electrode potential.

CO species at higher potentials. The increase of θ_2 was probably due to the competitive adsorption between O_2H and CO. The significant removal of CO at higher potentials led to more active sites available for O_2H adsorption, and thus, θ_2 increased with potential. Noteworthy was the large CO coverage, especially at lower potentials, which was associated with the strong adsorption strength of Pt with CO and indicated that the presence of methanol significantly reduced the active sites for the ORR at the DMFC cathode. The free active surface, also shown in Fig. 3, was quite small, which was consistent with the above analysis.

In order to show the methanol effect on the ORR more straightforwardly, the polarization curves were calculated and are presented in Fig. 4. Clearly, the polarization curve for simultaneous MOR and ORR showed significant lower performance than that for the pure ORR, which was calculated by assuming zero methanol concentration and CO coverage, especially at lower potentials. This result, consistent with the coverage variation, indicates that the presence of methanol greatly affected the ORR. The total effect of methanol on the ORR could be divided into two parts: the parasitic current effect, which assumed MOR and ORR independent of each other, and the poisoning effect, which was mainly due to adsorption of the CO species. To further clarify the methanol effect on ORR, the parasitic current effect and the total effect were respectively obtained from the partial MOR current density and the difference of the current densities between pure ORR and simultaneous MOR and ORR at the same potential. The ratio of parasitic current effect and total effect was plotted in the inset of Fig. 4. The ratio of parasitic current effect and total effect was below 0.1 at 0.65 V and then increased to over 0.5 at 0.75 V, revealing that the poisoning effect was dominant at low potentials while the parasitic current effect was more important at high potentials, which was consistent with the results in Fig. 3. These results indicate that the interaction between ORR and permeated methanol could not be explained by a classical mixed potential theory, especially at low potentials.

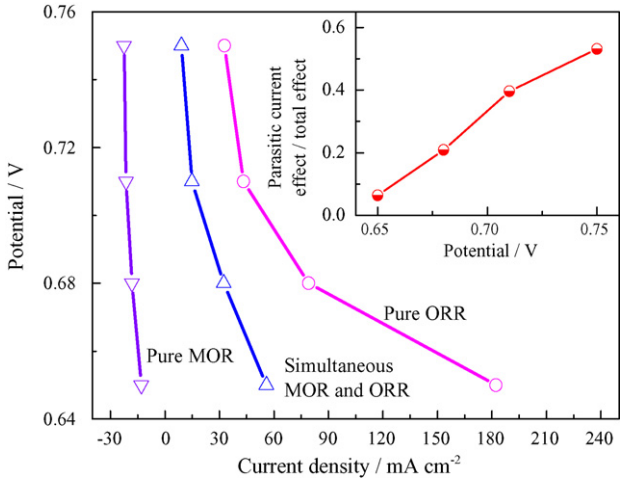

Fig. 4. Calculated polarization curves for pure ORR and simultaneous MOR and ORR at various potentials. Inset: the ratio of parasitic current and total effects of permeated methanol on ORR.

Methanol crossover through the membrane occurs mainly due to the driving forces of concentration gradients and electro-osmosis, which, at steady state, can be described by

$$D_M \left(\frac{\partial^2 c_1}{\partial x^2} \right) - \lambda \frac{I_F}{F} \frac{\partial c_1}{\partial x} = 0 \quad (27)$$

where D_M is the methanol diffusivity in Nafion membrane, λ the coefficient associated with electro-osmotic drag. This equation was solved to give the methanol permeation rates due to the concentration diffusion and the electro-osmotic drag. During the calculation, the values of 1.37×10^{-10} m^2 s^{-1} and 0.045 were used for D_M and λ, which were estimated from the limiting current density for methanol crossover through the Nafion membrane, as described by Ren et al. [7]. Fig. 5 shows the calculated methanol fluxes resulted, respectively, from the concentration diffusion and the electro-osmotic drag at various potentials. For the case of the electro-osmotic drag, the methanol flux decreased with increasing potential, due to lower cathodic current densities at higher potentials. For the case of the concentration diffusion, on the contrary, a slight increase of methanol flux with potential was observed, which could be explained in terms of the methanol concentrations at both sides of the half MEA. Apparently, the methanol concentration at the electrode side was reduced due to larger MOR rates, while the methanol concentration at the other side of the half MEA was almost maintained constant, at higher potentials. Hence, the methanol flux due to concentration gradient increased with potential. The increase of methanol flux due to concentration gradient with potential, however, was slight due to the small variation of the methanol concentration at the electrode side. It was interesting that, even at low potentials when cathodic current density was relatively larger, the methanol flux due to concentration diffusion was still significantly higher than that due to electro-osmotic drag, which revealed that the methanol flux due to the concentration diffusion was the dominant way for methanol crossover through the Nafion membrane. It should be noticed that this was just the observation in our case, and methanol fluxes due to concentration diffusion and electro-osmotic drag were highly dependent on the electrode design and operation condition.

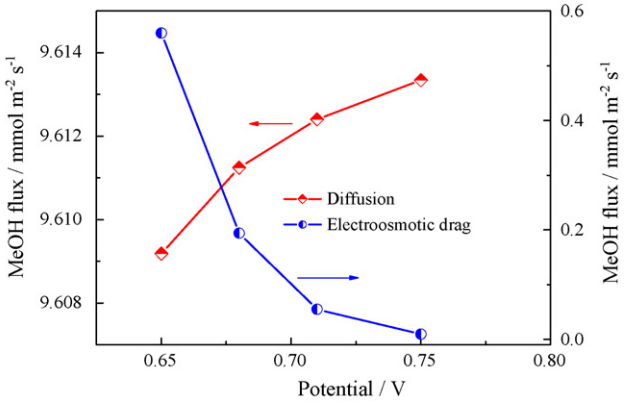

Fig. 5. Calculated methanol fluxes resulted from the concentration diffusion and electro-osmotic drag as a function of electrode potential.

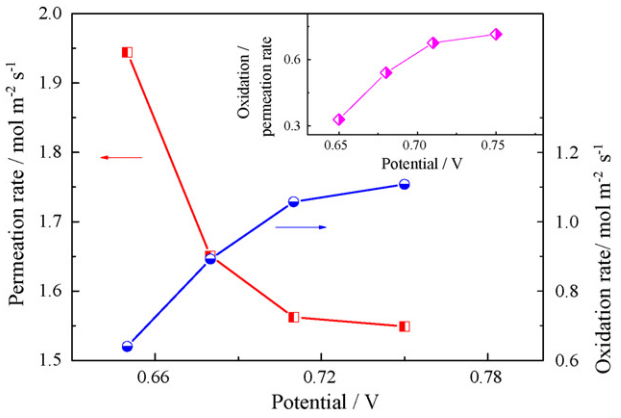

Fig. 6. The rate of methanol permeation through the membrane and the rate of methanol oxidation at the cathode as a function of electrode potential. Inset: the ratio of methanol oxidation and permeation rates.

The rate of methanol permeation through the membrane and the rate of methanol oxidation at the cathode as a function of the electrode potential were also calculated and are compared in Fig. 6. The rate of methanol permeation through the membrane decreased with increasing potential, which was the net result of both concentration diffusion and electro-osmotic drag as shown in Fig. 5. The rate of methanol oxidation, which is difficult to be measured by other electrochemical methods but can be easily obtained by this model-based EIS method, increased steadily with potential, due to faster MOR kinetics at higher potentials. The inset of Fig. 6 presents the ratio of the rate of methanol oxidation to that of methanol permeation. It is interesting to find that, at all potentials, the electrochemical oxidation rate was only 40–70% of the permeation rate, indicating that the permeated methanol could not be completely oxidized by electro-catalytic reaction at the DMFC cathode, even at high potentials. The non-electrochemically oxidized methanol may remain in its origin state, which was proved by some spectroscopic observations [29], or be oxidized by a chemical reaction, which was observed by Vielstich and coworkers [30,8]. No matter what form the nonelectrochemically oxidized methanol was, the assumption

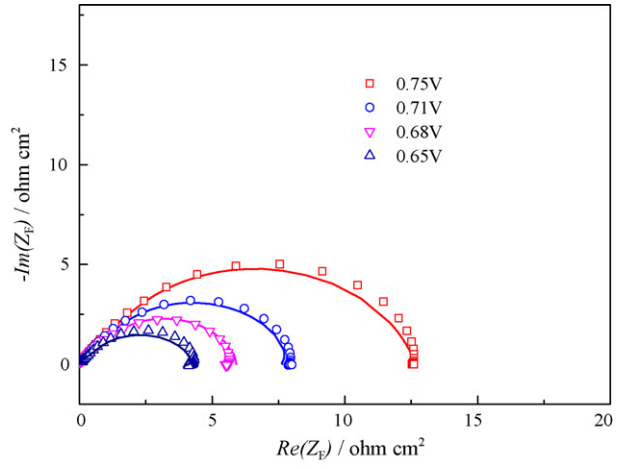

Fig. 7. Simulated EIS patterns based on the extracted kinetic parameters. Hollow points: experimental data, solid points: simulated plots.

that all permeated methanol could be completely oxidized by electro-catalytic reaction might lead to some errors in explaining experimental phenomena or mathematical modeling.

Finally, to verify the reliability of the model-based EIS approach and the accuracy of the calculated results, the EIS patterns calculated from the extracted parameters were compared with experimental results and are shown in Fig. 7. Clearly, agreements between the experimental and simulated results were observed, demonstrating the reliability of the method by the combining use of EEC method and a mathematical modeling.

5. Conclusions

The simultaneous MOR and ORR behavior at a DMFC cathode, resulted from methanol crossover, was investigated by a model-based EIS method that couples an EEC and a mathematical model derived from the detailed reaction kinetics. This method combines the advantages of the quantitative fitting of the experimental data in the EEC method and the exact physical equivalent for every parameter in the mathematical modeling, and can be easily implemented to extract the reaction details of the studied electrochemical systems. As far as we know, this is the first attempt to study the simultaneous MOR and ORR at a DMFC cathode by a model-based EIS method. Agreements between experimental and theoretical EIS data demonstrated the reliability of the model-based EIS method. Most of the detailed reaction information, e.g. kinetic parameters and state variables, about the DMFC cathode could be conveniently extracted out by this model-based EIS approach, which is very helpful to understand the cathode behavior. From the obtained parameters, some significant facts related to the DMFC cathode were revealed. The presence of methanol at the cathode could lead to a significant poisoning effect on the oxygen reduction reaction due to a high CO coverage, especially when the cathode operates at low potentials. In modeling the DMFC performance, it has usually been assumed that all permeated methanol can be completely oxidized by electrochemical reaction at the DMFC cathode. However, this work reveals that this assumption is questionable. Whether the permeated methanol can be completely oxidized by electrochemical reaction depends highly on the electrode design and operating conditions.

Acknowledgement

The work described in this paper was fully supported by a grant from the Research Grants Council of the Hong Kong Special Administrative Region, China (Project No. 622305).

References

[1] S. Zhou, T. Schultz, M. Peglow, K. Sundermacher, Phys. Chem. Chem. Phys. 3 (2001) 347.
[2] H. Dohle, J. Divisek, J. Mergel, H. Oetjen, C. Zingler, D. Stolten, J. Power Sources 105 (2002) 274.
[3] U. Paulus, T. Schmidt, H. Gasteiger, in: W. Vielstich, A. Lamm, H. Gasteiger (Eds.), Handbook of Fuel Cells, vol. II, Wiley, UK, 2003 (Chapter 38).
[4] Z. Jusys, R. Behm, Electrochim. Acta 49 (2004) 3891.

[5] B. Bittins-Cattaneo, S. Wasmus, B. Lopez-Mishima, W. Vielstich, J. Appl. Electrochem. 23 (1993) 625.
[6] D. Chu, S. Gilman, J. Electrochem. Soc. 141 (1994) 1770.
[7] X. Ren, T. Springer, T. Zawodsinski, S. Gottesfeld, J. Electrochem. Soc. 147 (2000) 466.
[8] V. Paganin, E. Sitta, T. Iwasita, W. Vielstich, J. Appl. Electrochem. 35 (2005) 1239.
[9] J. Müller, P. Urban, J. Power Sources 75 (1998) 139.
[10] P. Piela, R. Fields, P. Zelenay, J. Electrochem. Soc. 153 (2006) A1902.
[11] G. Li, P.G. Pickup, Electrochim. Acta 49 (2004) 4119.
[12] K. Furukawa, K. Okajima, M. Sudoh, J. Power Sources 139 (2005) 9.
[13] J. Diard, N. Glandut, P. Landaud, B. Gorrec, C. Montella, Electrochim. Acta 48 (2003) 555.
[14] X. Wang, I. Hsing, Y. Leng, P. Yue, Electrochim. Acta 46 (2001) 4397.
[15] C. Cao, Electrochim. Acta 35 (1990) 831.
[16] C. Cao, Electrochim. Acta 35 (1990) 837.
[17] J. Hu, J. Zhang, C. Cao, I. Hsing, Electrochim. Acta 49 (2004) 5227.
[18] X. Wu, H. Ma, S. Chen, Z. Xu, A. Sui, J. Electrochem. Soc. 146 (1999) 1847.
[19] Z. Jusys, R.J. Behm, J. Phys. Chem. B 105 (2001) 10874.
[20] U. Krewer, M. Christov, T. Vidakovic, K. Sundmache, J. Electroanal. Chem. 589 (2006) 148.
[21] O. Antonie, Y. Bultel, R. Durand, J. Electroanal. Chem. 499 (2001) 85.
[22] J. Diard, B. Gorrec, C. Montella, C. Montero-Ocampo, J. Electroanal. Chem. 352 (1993) 1.
[23] E. Antolini, L. Giorgi, A. Pozio, E. Passalacqua, J. Power Sources 77 (1999) 136.
[24] N. Jia, R. Martin, Z. Qi, M. Lefebvre, P. Pickup, Electrochim. Acta 46 (2001) 2863.
[25] T. Navessin, S. Holdcroft, Q. Wang, D. Song, Z. Liu, M. Eikerling, J. Horsfall, K. Lovell, J. Electroanal. Chem. 567 (2004) 111.
[26] M. Eikerling, A. Kornyshev, J. Electroanal. Chem. 475 (1999) 107.
[27] W. Lin, M. Zei, M. Eiswirth, G. Ertl, T. Iwasita, W. Vielstich, J. Phys. Chem. B 103 (1999) 6968.
[28] H. Hoster, T. Iwasita, H. Baumgartner, W. Vielstich, J. Electrochem. Soc. 148 (2001) A496.
[29] I.T. Bae, J. Electrochem. Soc. 153 (2006) A2091.
[30] W. Vielstich, V. Paganin, F. Lima, E. Ticianelli, J. Electrochem. Soc. 148 (2001) A502.